Analysis and multi-response optimization of two dew point cooler configurations using the desirability function approach

A. F. Boudjabi, Chadi Maalouf, T. Moussa, D. Abada, D. Rouag, M. Lachi, G. Polidori

Energy Reports 7 (2021) 5289–5304

Contents lists available at ScienceDirect

Energy Reports

journal homepage: www.elsevier.com/locate/egyr

Research paper

Analysis and multi-response optimization of two dew point cooler configurations using the desirability function approach

A.F. Boudjabi [a,b], C. Maalouf [c,*], T. Moussa [c], D. Abada [b,d], D. Rouag [b], M. Lachi [c], G. Polidori [c]

[a] Department of Mechanics, University of Oum El Bouaghi, 04000 Oum El Bouaghi, Algeria
[b] Energy & Environment Laboratory, University of Constantine 3 - Salah Boubnider, 25016 Ali Mendjeli, Algeria
[c] MATIM, University of Reims Champagne Ardenne, 51687 Reims cedex 2, France
[d] Department of Architecture, University of Oum El Bouaghi, 04000 Oum El Bouaghi, Algeria

ARTICLE INFO

Article history:
Received 19 November 2020
Received in revised form 11 August 2021
Accepted 18 August 2021
Available online 3 September 2021

Keywords:
Combined dew point cooler
Modeling
Desirability approach
Optimization
GenOpt
SPARK

ABSTRACT

Due to climate change and hot summers in most of Algeria's regions, air conditioning has become a thorny issue, resulting in excessive energy consumption. This research focuses on the implementation of dew point evaporative coolers as an alternative to conventional air conditioners. The desirability function approach is used to predict the optimal operating parameters and compare the thermal performance and water consumption of two dew point cooler configurations (counter flow-regenerative cooler and combined parallel–regenerative cooler) under different climatic conditions in Algeria. A numerical model is developed and validated using literature data for regenerative and combined dew point evaporative systems. Parametric analysis and multi- to single-objective optimization simulations were performed with the GenOpt simulation software, identifying the most influential parameters and predicting the optimal conditions for both configurations. The findings suggest that the optimal channel spacing, working air ratio, and primary air velocity are identical for both technologies.

However, the cooling capacity and the coefficient of performance of the combined parallel–regenerative cooler are higher in drier climates. When both technologies are compared at nearly equal dew point efficiency, the combined configuration improves cooling capacity by 5%, while increasing water consumption by about 40%. This study provides a useful method for assessing cooling capacity and adapting suitable dew point technology to various climates and cities.

1. Introduction

Current demographic trends confirm that most countries have undergone significant social and energy consumption shifts in the last few decades. Current air conditioning systems have high electricity consumption and harmful global warming potential. Buildings account for 42% of energy consumption in Algeria (Maalouf et al., 2018), with a growth of +1.9% from 2015 to 2016 and +17.6% from 2017 to 2018 (Algerian Energy Ministry, 2017, 2019). The air-conditioning sector, in particular, is growing rapidly. Evaporative coolers are a promising technology and a viable alternative to conventional vapor compression systems, which are widely used worldwide (Anisimov and Pandelidis, 2015). Indeed, traditional evaporative coolers actually have some drawbacks in terms of humidity for direct systems and limited efficiency for indirect systems (Camargo et al., 2003; Lertsatitthanakorn et al., 2006; Stoitchkov and Dimitrov, 1998). In each case, the supply air temperature may not be lower than the wet bulb temperature of the ambient air.

Sub-wet bulb evaporative coolers are more attractive and can be both energy efficient and environmentally friendly (Boukhanouf et al., 2014). They produce a higher cooling capacity with low energy consumption by providing a supply temperature close to the air dew point temperature (Zhao et al., 2008). The system is a heat and mass transfer exchanger with dry and wet channel pairs in a stack, separated by a wet return surface. This is a modified indirect evaporative configuration that keeps the supply air temperature lower than the wet bulb air temperature (Zhan et al., 2011). In the IEC indirect evaporative cooler, the supply air enters the dry channel and transfers its sensible heat to the working air due to water film evaporation as shown in Fig. 1, with the two air streams being separated (Riangvilaikul and Kumar, 2010; Ren and Yang, 2006). In the regenerative evaporative cooler (Maalouf et al., 2018; Maisotsenko et al., 2003; Liu et al., 2019), the difference with the previous system occurs at the end of the dry channel, where some of the primary air returns to the wet channel as working air, to recover the heat transferred to the water film through the separation medium (see Fig. 2).

* Corresponding author.
E-mail address: chadi.maalouf@univ-reims.fr (C. Maalouf).

https://doi.org/10.1016/j.egyr.2021.08.128

Nomenclature

$\dot{m}$	Airflow rate, kg/s
C_p	Specific heat capacity, J/(kg K)
T	Temperature, K
t	Air temperature in the wet channel, K
x	Streamwise coordinate along channel, m
U	Overall heat transfer coefficient, (W/(m^2 K)
h	Convective heat transfer coefficient, (W/(m^2 K)
g	Air moisture content, kg/kg
D	Channel width/depth, m
H	Channel height/gap, m
l	Channel length, m
f	Darcy friction factor
D_h	Hydraulic diameter, m
v	Air velocity, m/s
Δp	Pressure drop, Pa
P	Power/energy consumption, W
WAR	Working air ratio
PAR	Volumetric flow rate, m^3/s
$\dot{V}$	Parallel air ratio
$\dot{Q}$	Cooling capacity, W
COP	Coefficient of performance

Subscripts

d	Dry channel
a	Wet channel
ν	Vapor
fw	Water film
wb	Wet bulb
dp	Dew point
w	Working air
Le	Lewis number
Re	Reynolds number
Pr	Prandtl number
Nu	Nusselt number
dev	Limit of undeveloped airflow region
1st	1st Order boundary conditions
2nd	2nd Order boundary conditions
in	Dry channel inlet
out	Dry channel outlet
f	Fan
pp	Parallel part of the cooler
regp	Regenerative part of the cooler
t	Total

Special characters

ρ	Air density, Kg/m^3
ε	Cooling efficiency
ζ	Local pressure drop coefficient
η	Device efficiency

Another arrangement consists of a combined parallel-flow and regenerative indirect evaporative cooler (see Fig. 3). Ambient air enters in a parallel section in the wet channel and in the dry channel; a part is extracted at the end of the dry channel and

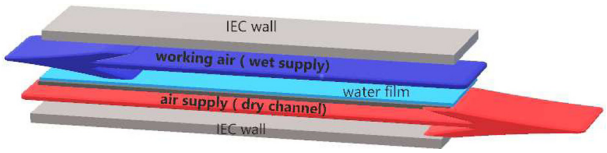

Fig. 1. Indirect evaporative cooler IEC.

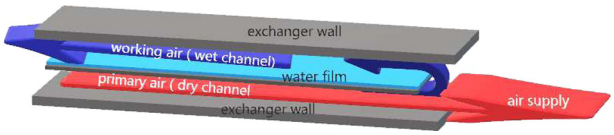

Fig. 2. Dew point evaporative cooler (counter flow-regenerative).

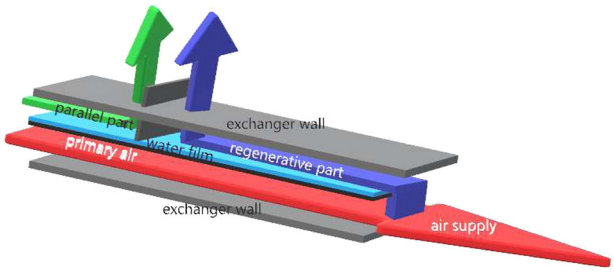

Fig. 3. Parallel–regenerative evaporative cooler.

diverted back in counter flow into the regenerative section of the wet channel. This set up provides high cooling efficiency (Anisimov and Zuchowicki, 2005; Hasan, 2010).

In the literature, the dew point cooler has been extensively studied for design and operating parameters in order to achieve optimal air supply temperature, dew point efficiency, and cooling capacity. However, the studies differ in system design or numerical model used. The results of these different models are validated by experimentation under different climatic conditions and operating parameters. Hasan (2010) performed a 1D numerical study of four evaporative coolers with one and two stages, under co-current, counter-current or cross-flow configurations. The author achieved 116% wet bulb efficiency for an indirect stage with wet return surface. In another study, Riangvilaikul and Kumar (2010) conducted a numerical and experimental study of a vertical configuration of the dew-point evaporative system for different conditions. Their results show that with an air velocity less than 2.5 m/s, a channel gap of less than 5 mm, a channel length more than 1 m, and a working air ratio of about 35%–60%, a wet bulb efficiency of more than 100% can be achieved. Lee and Lee (2013) used a counter-current system with a return air ratio; they performed the model using an aluminum plate supporting a wet media to activate heat transfer. For an air inlet temperature of 30 °C and a relative humidity of 50%, they obtained a supply air temperature of 22 °C. A three-dimensional numerical study of the laminar airflow of a counter-current evaporative cooler was also proposed by Pengfei and Xinyu (2015). The authors used Ansys software to simulate a dry channel for product air, a wet channel and a dry channel for the working air with holes on the wet return medium. They obtained a dew point efficiency of 71.2%. In a 3D numerical simulation using the C++ language, Jafarian et al. (2017a,b) considered a modified boundary condition on the separator wall surface. Their results predicted a prototype performance of about 3.5% and the authors deduced a maximum error between 2D and 3D models of less than 4.5%. Guangya et al. (2019) identified the parameters influencing the

M-cycle exchanger and proposed a correlation of the dew point efficiency. The deviations between numerical simulations and experimental were 2.35%. Pakari and Ghani (2019) examined the cooler using a 1D model and a 3D simulation with COMSOL Multiphysics and showed that the numerical results agreed well with the experimental results with a discrepancy of 8.5% and 10% respectively. Ham and Jeong (2016) proposed a finite difference model of a dew point exchanger (DPHX), where the designed device has two inlets and two outlets. The authors found that the air supply in dry channel of an M- cycle evaporative cooler leads to the limitations of complex ventilation control and wasted dehumidification energy. Calculations of cooling performance and pressure drop reveal that the DPHX can reduce energy consumption by 15% compared to the M- cycle system by reducing the size of the liquid desiccant unit and fans. Anisimov et al. (2014) considered in their study an original mathematical model based on the modified ε-NTU method. Numerical simulations were used to determine the following optimal design parameters: inlet air temperature, cooling capacity, NTU number. Five different heat exchanger arrangements were analyzed, two being original designs. Their results indicated that the exchangers are most efficient in hot and dry climatic conditions. In their new cross flow HMX, the high effectiveness is related to the temperature distribution of the inlet working air in the wet channel. In another study, Anisimov et al. (2015) performed a 2D numerical simulation and an optimization of a combined indirect evaporative cooler. The results were validated with experimental data and the exchanger achieved higher cooling capacity and lower supply air temperatures. Pandelidis et al. (2017) used numerical simulations to describe three advanced indirect evaporative coolers. Two new combined heat exchangers, proposed by the authors, were compared to the cross flow M-cycle exchanger. The results showed that in the parallel part, the heat transfer rate increases and leads to a higher overall cooling efficiency. The combined cross regenerative cooler is the most favorable solution, with a higher energy efficiency factor and simpler design. Numerical models validated by experimental data allow to evaluate the performance of the system and to determine the optimal operating conditions and parameters that enhance it under different climatic conditions. This approach is quite relevant for dew point evaporative coolers, given the significant impact of design and operating conditions.

Jafarian et al. (2017a,b) conducted a modeling and optimization study of a dew-point counter flow IEC based on a 2D numerical model developed using openFOAM software and a multi-objective mathematical algorithm (group method of data handling (GMDH)) type based on a polynomial neural network. The authors performed calculations for three Iranian climate regions. The optimal values of the decision variables lead to maximize the energy efficiency factor COP and minimize the specific area of the cooler. As a result of the optimization, the improvements in these two parameters for the warm climate city were 36.3% and 30.9% respectively, while they were about −2.63% and 16% in the warm-semi humid climate and 2.19% and 7.92%, in the warm–humid climate. In the study of Lin et al. (2020), a two-dimensional model of a dew point evaporative cooler is performed using a CFD simulation and validated by experimental measurements with a discrepancy of about 4.7%. The model is coupled with a multi-objective and a multi-to-single objective optimization. The results revealed that the multi-to-single-objective optimization using a desirability function is accurate for studying decision variables and objective functions. In addition, the optimization approach can improve the system performance by 36%–92% of the COP. Sohani et al. (2018) performed a comparative study and optimization analysis concerning the performance evaluation of counter-regenerative and cross flow dew point evaporative coolers coupled to a small-scale residential building under four different climatic conditions (according to Köppen–Geiger classification). The authors showed that, in the performance optimization, economic and climatic parameters have an impact on the working air ratio and the cooler length. Compared to the base case conditions, a 64.4% and 86.4% decrease in life cycle cost and annual water consumption was obtained, and a 1039% increase in annual average of COP was achieved for the optimal design.

Earlier investigations on the energy performance of dew point evaporative cooling are extremely important. Mathematical models were proposed to physically describe the cooling process and have been shown to be sufficiently accurate. The system performance is improved by optimization. However, analysis and comparison between different cooler configurations is still lacking as well as data on system water consumption, which is important information in arid climates. Therefore, to address these issues and based upon the literature findings, two systems are selected in the present study and compared by optimization for three Algerian cities with different climatic conditions. These systems are the regenerative configuration and the combined parallel and counter one. While the first configuration is widely studied in the literature, few authors have studied the second (Hasan, 2010; Anisimov et al., 2015; Pandelidis et al., 2017). The comparison focuses on the optimized performance factors: dew point efficiency, COP, and system cooling capacity. For the optimization, the desirability approach is applied using GenOpt tool. In the first part, the mathematical models are presented and implemented in the SPARK simulation environment. Then, the models are validated based on literature data. Furthermore, using the hybrid GPS/PSO algorithm, optimization is performed and allows to identify the optimal level of input design parameters for the different configurations. The results are presented for the different cities and detailed only for the city of Constantine. The critical parameters are also identified by simulation and the theoretical water consumption is computed. The results for both configurations are compared. The findings from this study allow a better understanding of the key design parameters of dew point evaporative coolers and the interaction of performance factors.

2. Mathematical model

Using a one-dimensional simulation, the system is divided into computational cells, one element of which is shown in Fig. 4. To simplify the mathematical equations, the following assumptions are considered:

- No heat transfer between the system and the surroundings.
- The heat transfer fluxes are perpendicular to the airflow in the channels.
- The gap or height of channels is small compared to their length, so that the flow is assumed to be unidirectional.
- The water film distribution is homogeneous over the entire surface of the wet plate (the water film is on both upper and lower surfaces of the wet channel).
- The airflow is defined as an incompressible gas.
- The airflow is considered laminar due to low velocities ($Re_H < 2000$).

2.1. Energy conservation balance

The energy conservation balance for the airflow through a cell element in the dry channel part is given by:

$$\frac{\dot{m}_d C_{pa}}{D}\frac{dT_d}{dx} = -U_d(T_d - T_{fw}) \quad (1)$$

where (T_d) is the air dry bulb temperature in the dry channel, (T_{fw}) the water film temperature, (U_d) the overall heat transfer

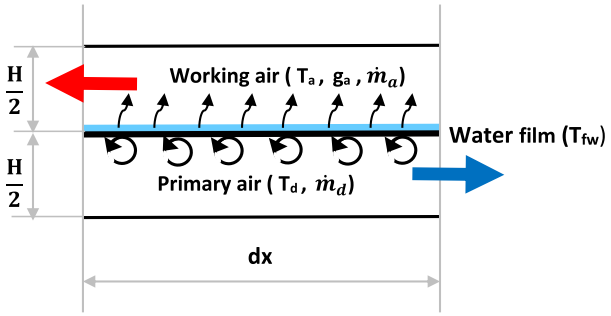

Fig. 4. Computational cell element.

coefficient between the dry channel and the water film and ($\dot{m}_d$) the airflow rate in the dry channel.

The energy conservation balance for the airflow in the wet channel is expressed as:

$$\frac{\dot{m}_a C_{pa}}{D}\frac{dt_a}{dx} = -h_{aw}\left(T_{fw} - t_a\right) - \rho\, h_m \left(g_{fw} - g_a\right) C_{pv} t_a \tag{2}$$

where: (t_a) is air dry bulb temperature in the wet channel, (g_a) humidity ratio of air, (g_{fw}) humidity ratio at saturation near water film, ($\dot{m}_a$) airflow rate in the wet channel, (h_{aw}) heat transfer coefficient in the wet channel and (h_m) convective mass transfer coefficient between the wet airflow and the water film surface.

These heat transfer parameters are related by the Lewis relation:

$$\frac{h_{aw}}{h_m} = \rho C_p Le^{2/3} \tag{3}$$

The mass conservation equation of air in the wet channel gives:

$$\frac{\dot{m}_a}{D}\frac{dg_a}{dx} = -\rho h_m \left(g_{fw} - g_a\right) \tag{4}$$

The coupled energy balance of dry and wet airflow in the cell element on the media between the channels gives:

$$\frac{\dot{m}_{fw} C_{pfw}}{D}\frac{dT_{fw}}{dx} = -U_d\left(T_d - T_{fw}\right) + \rho h_m \left(g_{fw} - g_a\right) h_{fg} + h_{aw}\left(T_{fw} - t_a\right) \tag{5}$$

2.2. Nusselt number correlations

The heat transfer coefficients are calculated from the Nusselt number. For laminar flow through a rectangular duct, the gap H is considered as the specific dimension, Reynolds number Re_H is referred to this dimension and the Nu correlations are for two regions: the undeveloped zone ($l < l_{dev}$) and the fully developed zone. The length limiting the two zones is defined by Eq. (6) (Zhao et al., 2008; Anisimov et al., 2014):

$$\frac{l_{dev}}{D_h} = 0.05 Re_H Pr \tag{6}$$

In the undeveloped flow region, Nusselt number is calculated from empirical expressions of first-order (constant wall temperature) and second- order (constant heat rate) boundary conditions respectively (Anisimov et al., 2014):

$$Nu_{1st} = 1.533\left(Re_H Pr \frac{H}{l}\right)^{1/3} \tag{7}$$

$$Nu_{2nd} = 1.755\left(Re_H Pr \frac{H}{l}\right)^{1/3}$$

For the developed airflow region, the Nusselt number is set constant and equal to (Anisimov et al., 2014):

$$Nu_{1st} = 3.77 \tag{8}$$

Table 1
Local pressure loss coefficients (Sohani et al., 2018; Duan, 2011).

Airflow	Coefficient	Local pressure drop	value
Dry channel	ζ_1	Inlet contraction	0.5
	ζ_{1-2}	Line flow	0.1
	ζ_2	Outlet expansion	1.0
Wet channel	ζ_1	Inlet contraction	0.5
	ζ_{1-3}	Branch flow	0.9
	ζ_{3-4}	Diversion	1.5
	ζ_4	Working air outlet expansion	1.0
Parallel wet channel	$\zeta_{1'}$	Inlet contraction	0.5
	$\zeta_{2'-3'}$	Diversion	1.5
	$\zeta_{4'}$	Parallel outlet expansion	1.0

$$Nu_{2nd} = 4.12$$

2.3. Wet bulb and dew point efficiencies

The wet bulb efficiency is defined from Eq. (9) and the dew point efficiency is given by Eq. (10), (Maalouf et al., 2018; Zhao et al., 2008; Lin et al., 2020).

$$\varepsilon_{wb} = \frac{T_{d,out} - T_{d,in}}{T_{wb} - T_{in}} \tag{9}$$

$$\varepsilon_{dp} = \frac{T_{d,out} - T_{d,in}}{T_{dp} - T_{d,in}} \tag{10}$$

2.4. Exchanger cooling capacity and coefficient of performance (COP)

Similarly, cooling capacity and coefficient of performance contribute to system performance through pressure drop, fan consumption, and cooling air production. Therefore, it is necessary to calculate both the cooling capacity and COP.

2.4.1. Pressure drop calculation

For fully developed laminar flow in non-circular ducts, the friction factor is calculated using the Reynolds number based on hydraulic diameter D_h (Eq. (11)). In the exchanger, the channel aspect ratio H/l nears zero, so, the relations used in the calculations are therefore (Anisimov and Pandelidis, 2015; Zhan et al., 2011; Holman, 2010):

$$D_h = \frac{4H.l}{2(H+l)} \text{ and } f = \frac{96}{Re_{D_h}} \tag{11}$$

The total pressure drop/head loss yields to friction losses along the channels (Eq. (12)) and local pressure losses (Eq. (13) and Table 1) as shown in the following relationships (Zhao et al., 2008; Jafarian et al., 2017a,b; Kashyap et al., 2020):

$$\Delta p_{friction} = f\frac{l.\ \rho.\ v^2}{D_h\ 2} \tag{12}$$

$$\Delta p_{local} = \sum \zeta \frac{\rho.\ v^2}{2} \tag{13}$$

2.4.2. Fan power

The actual fan power is deduced from Eq. (14) (Zhao et al., 2008; Jafarian et al., 2017a,b; Kashyap et al., 2020):

$$P_f = \frac{\Delta p_w.\dot{V}_w + \Delta p_{pp}.\dot{V}_{pp} + \Delta p_d.\dot{V}_d}{\eta_f} \tag{14}$$

where Δp_d and $\dot{V}_d$ are the pressure drop and volumetric flow rate in the dry channel, Δp_w and $\dot{V}_w$ are the pressure drop and volumetric flow rate of working air in the regenerative part respectively. η_f is the fan efficiency taken equal to 0.55.

Table 2
System parameters.

	Reference	Range
Inlet air temperature	35 °C	30–40 °C
Air moisture content	11 g/kg	11 g/kg
Intake air velocity	2 m/s	1.11–2 m/s
Working air ratio	0.33	0.22–0.79

Δp_{pp} and $\dot{V}_{pp}$ are the pressure drop and volumetric flow rate in the parallel part of the combined arrangement, set to zero for the regeneration case.

2.4.3. Cooling capacity

The cooling capacity is expressed by (Zhao et al., 2008; Lin et al., 2020):

$$\dot{Q} = \dot{m}_d(1 - WAR)C_p\left(T_{d,in} - T_{d,out}\right) \quad (15)$$

where WAR is the working air ratio, defined as the ratio between the air flow in the regenerative wet channel and the primary air flow in the dry channel. C_p is the air specific heat with $T_{d,in}$ and $T_{d,out}$ being the inlet and outlet air temperatures respectively in the dry channel.

2.4.4. Coefficient of performance

The coefficient of performance COP is the ratio between the cooling capacity Eq. (15) and the total power consumption in the system and it is expressed by (Zhao et al., 2008; Jafarian et al., 2017a,b; Lin et al., 2020; Duan, 2011; Kashyap et al., 2020):

$$COP = \frac{\dot{Q}}{P_t} \quad (16)$$

The total energy consumption P_t includes fan power P_f and other devices consumption as motor pump and thermostat which is assumed to be constant.

To perform simulations under different climatic conditions and determine the optimal parameters for both cooler configurations, the present mathematical model is implemented using the finite difference method in the SPARK environment (Sowell and Haves, 2001). The following section focuses the validation of this implementation.

3. Model validation

The mathematical model developed in this study is validated by data from literature for both configurations. In this section, validation is presented using experimental results (Lin et al., 2020) for the regenerative cooler as well as numerical data (Hasan, 2010) for the combined configuration. The numerical model is also developed for the vertical arrangement of a dew point evaporative cooler validated by Riangvilaykul et al. (2010) study and the combined parallel–regenerative cooler is validated by the data of Pandelidis et al. (2017). Both validation details are presented in Appendix.

3.1. Horizontal counter flow dew point evaporative cooler

The numerical results presented in this section are based on measurements performed by Lin et al. In this case, the arrangement is horizontal and composed of ten pairs of dry and wet channels of 600 × 150 × 3 mm^3 each one (Fig. 5).

The parameters used for calculation are reported on Table 2.

In this case study, the effects of inlet primary air temperature, air velocity, working air ratio on supply air temperature, working air temperature, and total pressure drop were studied.

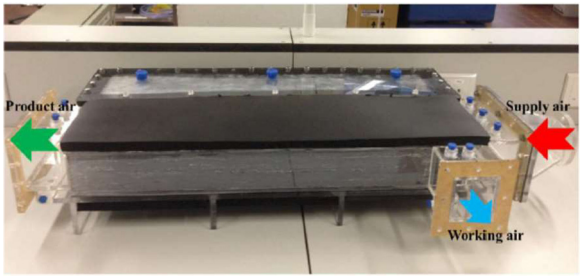

Fig. 5. Lab-scale exchanger (Lin et al., 2020).

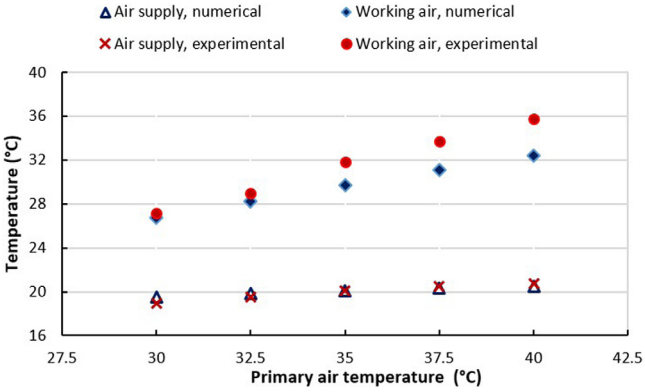

Fig. 6. Effect of primary air temperature on air supply and working air temperatures.

3.1.1. Effect of inlet air temperature

Fig. 6 shows the supply and working air temperatures as a function of the primary air inlet temperature. The primary air temperature varies from 30 °C to 40 °C, while the other operating parameters are set to their reference values (see Table 1). For the supply air temperature, the experimental and numerical values coincide sufficiently with a deviation ranging from 0.04% to 2.8%, corresponding to a difference in temperature less than 0.8 ° C. For the working air outlet temperature, a numerical to experimental difference of 2 °C to 4 °C is observed for primary air temperatures higher than 35 °C and an average deviation of 5.6%. However, the discrepancy remains acceptable.

3.1.2. Pressure drop

As plotted in Fig. 7, the pressure drop is expressed in terms of the primary air velocity in both channels. For higher flow rates, the air resistance is higher and requires more power consumption from the fan. The results of the numerical model are compared with the experimental results. The pressure drops predicted by the model are in a good agreement with the measured values with an average deviation of 3.3% for the dry channel and 5.3% for the wet channel.

Besides, the working air ratio in the wet channel also affects the flow resistance (see Fig. 8). The pressure drop increases in the wet channel and decreases in the dry channel for higher ratios (> 0.5), due to the airflow rate delivered in both channels. More than 50% of the primary flow rate is used for regeneration.

The model predictions agree well with the measurements and the average deviation in the dry channel is 6.7% with a difference of 0.12 Pa for a working air ratio of 0.22 to 3.23 Pa for a ratio of 0.7, while in the wet channel the deviation is about 1.7%.

More results of this validation case are presented in Appendix A.1, concerning inlet air velocity and working air ratio.

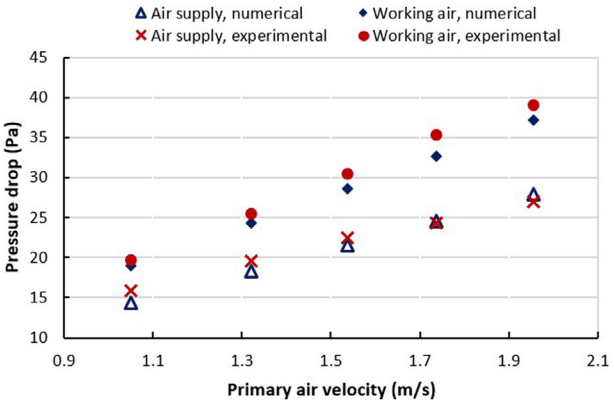

Fig. 7. Effect of primary air velocity on the air pressure drop.

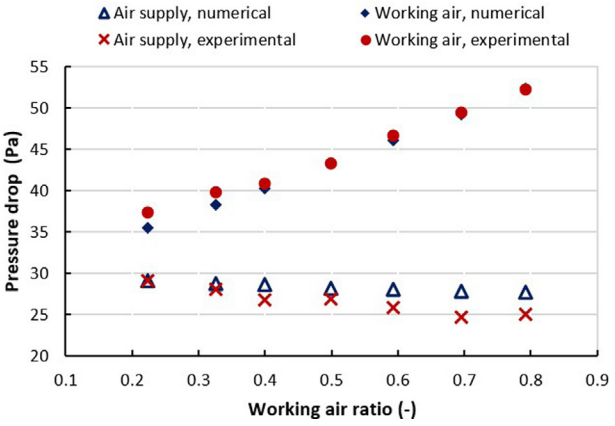

Fig. 8. Effect of working air ratio on the air pressure drop.

Table 3
Case parameters.

Channel's length	500 mm
Channel's width	500 mm
Channel's gap	3.5 mm
Primary airflow rate	0.0014 kg/s
Parallel airflow ratio	0.825
Working airflow ratio	0.452

3.2. Combined parallel–regenerative evaporative cooler

In this case, the results are validated with those given by Hasan (2010) whose details are shown in Fig. 9. The following air inlet conditions are assumed: air inlet temperature of 30 °C and moisture content of 9 g/kg. The specifications for this case study are presented in Table 3.

Figs. 10 and 11 show results from the SPARK model compared to Hasan's results. In the parallel flow part, the model yields an air supply temperature reaching 24.25 °C then decreasing to 15.59 °C at the end of the passage length, whereas the values in the data are 24.1 °C in the parallel part and 15.3 °C at the outlet. It is clear that a good agreement is found with Hasan's results. The error is about 1.26%. It can be seen that in the parallel part, the flow is characterized by a small variation in the water film temperature. Moreover, in the wet channel, the air properties are similar to those observed under adiabatic humidification conditions. In the regenerative part, the water film profile is different and the sensible heat transfer in the wet channel is characterized by two different active zones with opposite heat flux directions (before and after 90% of the channel length where the working air temperature reaches a minimum).

Table 4
Variation range of decision variables.

Decision variables	Unit	Minimum	Maximum
Length	mm	600	800
Width	mm	375	500
Gap height	mm	3	10
Working air ratio (WAR)	–	0.1	0.5
Inlet air velocity	m/s	1.5	3.5
Parallel air ratio (PAR)	–	0.1	0.9
Lparallel	–	0	0.66

4. Performance multiple response optimization

The heat and mass transfer process in dew point coolers is complex and its performance is defined by multiple factors or responses which are generally contradictory and must be optimized simultaneously. Identification of the optimal conditions for the input variables requires simultaneous consideration of all responses. This is called a multi-response optimization problem and can be solved using several approaches such as the desirability approach used in this study. This is a powerful tool used in multi-response systems. It is based on the transformation of all the responses obtained at different scales into a scale-free value. For each response $Y_i(x)$, an individual desirability function $d_i(Y_i)$ is assigned a number between 0 and 1. The value zero is assigned when the factors give an undesirable response, while the value 1 corresponds to the optimal performance for the factors under consideration. The individual desirabilities are then combined using the geometric mean, resulting in the overall desirability D:

$$D = (d_1 d_2 \dots d_n)^{1/n} = \left(\prod_{i=1}^{n} d_i\right)^{\frac{1}{n}} \tag{17}$$

The problem is then solved by maximizing the overall desirability. For each factor, individual desirability is calculated according to Derringer and Suich (1980) methodology to maximize each response:

$$d = \begin{cases} 0 & if\ (y < L) \\ \left(\dfrac{y-L}{T-L}\right)^{r} & if\ (\ L \le y \le T) \\ 1 & if\ (y > T) \end{cases} \tag{18}$$

where L and T are the lower limit and target value of y respectively. The factor r is a weight factor that can be set > 1, <1 or $= 1$ (linear function). In this study r is equal 1.

The literature has extensively studied the key performance factors of dew point coolers. Three main factors are determined: dew point efficiency, cooling capacity, and COP. For each factor the individual desirability is computed, and then overall desirability is calculated according to Eq. (17) with n = 3 which means that all factors have the same weight.

4.1. Decision variables

The geometric and operating conditions of the cooler are used as decision variables: channel gap, channel width, channel length, working air ratio (WAR) and inlet air velocity. For the combined cooler, additional variables are used: parallel air ratio (PAR) defined as the ratio of the working to primary air flow ratio in the parallel flow section, and Lparallel, which is the relative length of parallel part to the total cooler length (Table 4). The duct materials and thickness are those chosen by Lin et al. (2020).

For the outdoor conditions, three cases representative of the climatic conditions in Algeria are chosen as shown in Table 5. For each city, the regenerative cooler is optimized and compared to a reference case and then the combined cooler is optimized and compared to the optimal case of the regenerative cooler.

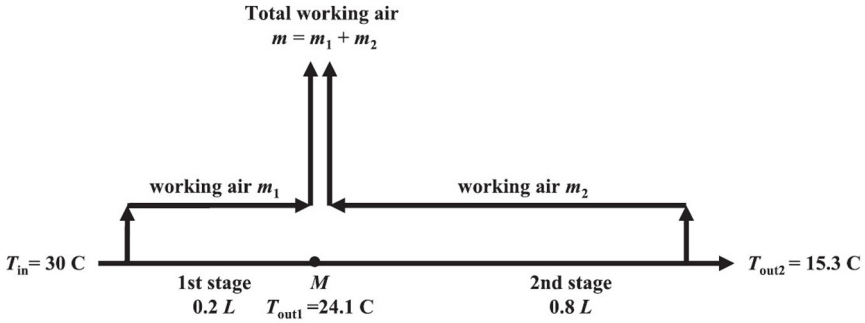

Fig. 9. Schematic airflow in a combined parallel–regenerative evaporative cooler (Hasan, 2010).

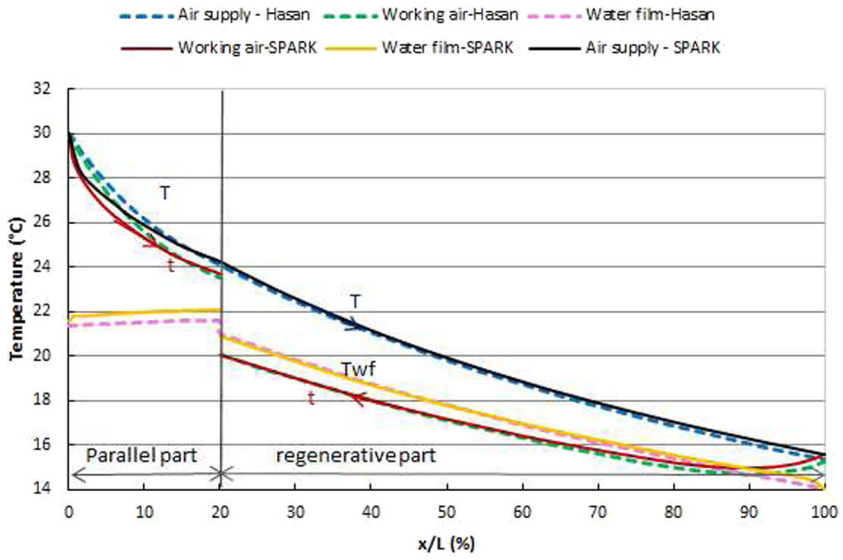

Fig. 10. Comparison of temperature profiles for air supply, working air and water film for the combined parallel–regenerative cooler.

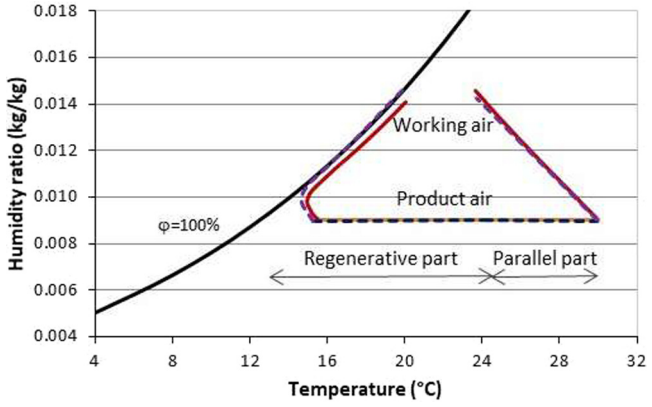

Fig. 11. Comparison between Hasan model (dashed lines) and SPARK results for air supply and working air conditions on the psychometric chart.

4.2. Constraints

Two constraints are imposed on the optimization problem as listed below:

– A constant exchange surface is imposed to compare different solutions while ensuring a similar manufacturing cost for coolers:

$$A = L * w = cte \tag{19}$$

Table 5
Ashrae summer design conditions (2%) of the selected cities.

	Climate	Elevation (m)	DBT (°C)	WBT (°C)	DBT–DPT (°C)
Ouargla	Hot desert	150	43.8	22.6	31.94
Constantine	Hot summer Mediterranean	690	35	19.8	23.02
Algiers	Hot summer Mediterranean	25	32	22.5	13.64

– The number of air channel pairs is 50 for the reference case.

The provided cooling capacity Q_{room} of the optimized cooler should be greater than the cooling capacity of the reference system which can be written as:

$$\dot{m}_{s,ref} C_p \left(1 - WAR_{s,ref}\right)\left(26 - T_{s,ref}\right) \leq \dot{m}_{opt,opt} C_p \left(1 - WAR_{s,opt}\right)\left(26 - T_{s,opt}\right) \tag{20}$$

Building indoor temperature is assumed to be 26 °C.

5. Methodology

To solve the problem, the optimization program GenOpt for minimizing a cost function evaluated by an external simulation program (SPARK in this work), is used. Such a program can be coupled to any simulation program that reads its input from text files and writes its output in text files (like EnergyPlus, TRNSYS, Dymola, SPARK…). Different files must be prepared to establish the communication between GenOpt and SPARK, as shown in

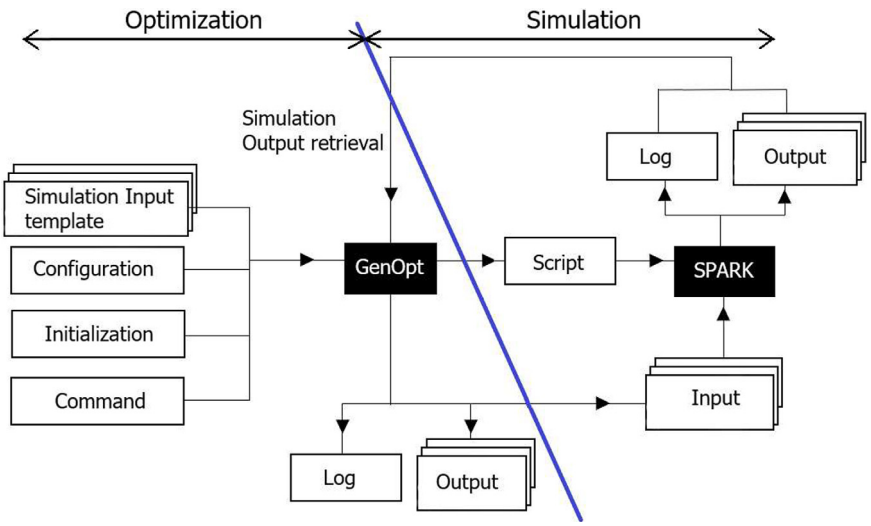

Fig. 12. Data flow of GenOpt–SPARK coupling.

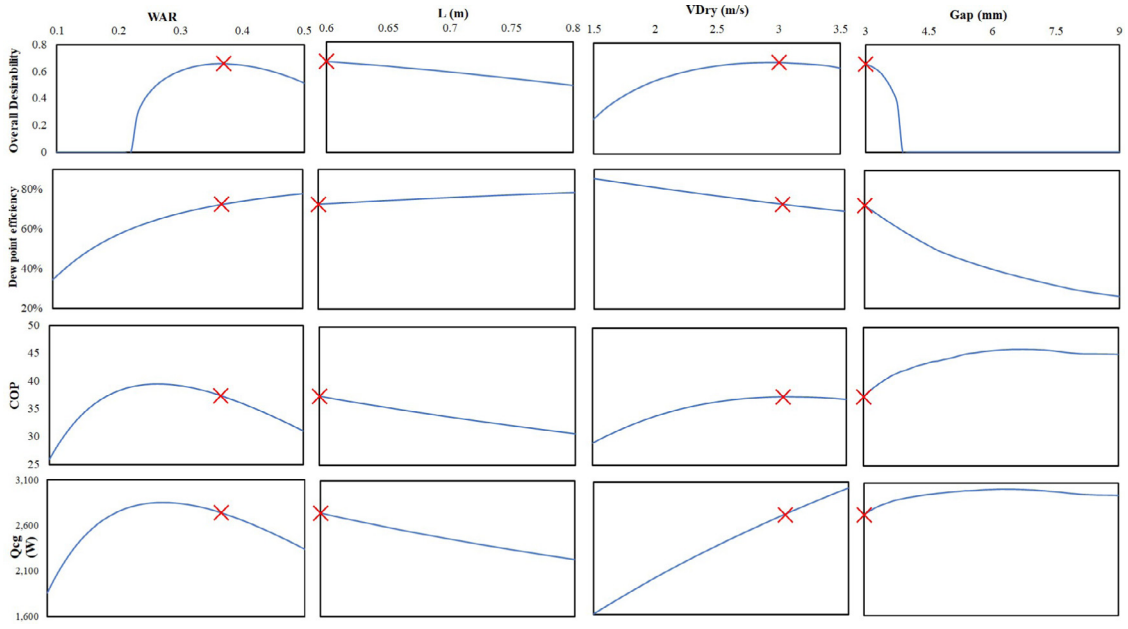

Fig. 13. Multiple response optimization using desirability function for Constantine city for the regenerative dew point cooler.

Fig. 12. An extensive overview on the details concerning the file preparations can be found in Wetter (2009) and can be summarized in Wetter (2000): GenOpt reads the simulation input template files, which are the simulation input files where the numerical value of each independent parameter is replaced by its variable name. Then it replaces these variable names with numerical values (determined by the chosen optimization algorithm) and writes the simulation input files. Afterwards, GenOpt starts SPARK (via commands written in the batch file), waits until the simulation is completed and then reads the simulation log files and the simulation output files. The simulation log files indicate any eventual error. If not, GenOpt looks for the value of the objective function in the simulation output files. An initialization file tells GenOpt where all files are located. The command file lists the independent parameters and their bounds. It also specifies which algorithm should be selected from GenOpt's algorithm library to perform the optimization. The configuration file tells GenOpt which messages in the log file indicate a simulation error, and how GenOpt should start the optimization. In this paper, the hybrid GPS/PSO algorithm is used. It is applicable for optimization problems with continuous parameters only, or mixed continuous and discrete parameters. It starts by performing a Particle Swarm Optimization (PSO) on a mesh, for a user-specified number of generations.

Then, it initializes the Hooke–Jeeves Generalized Pattern Search (GPS) algorithm, using the continuous independent variables of the particle with the lowest cost function value. The GPS starts with the best iteration found by the PSO algorithm and refines the search.

6. Results

6.1. Regenerative dew point cooler for Constantine city

Fig. 13 shows that the optimal values of dew point efficiency, COP, and cooling capacity are 72.5%, 38 and 2750 W respectively for an overall desirability value of 0.66. These values are evaluated for WAR of 0.36, an exchanger length of 0.6 m, a dry air velocity of

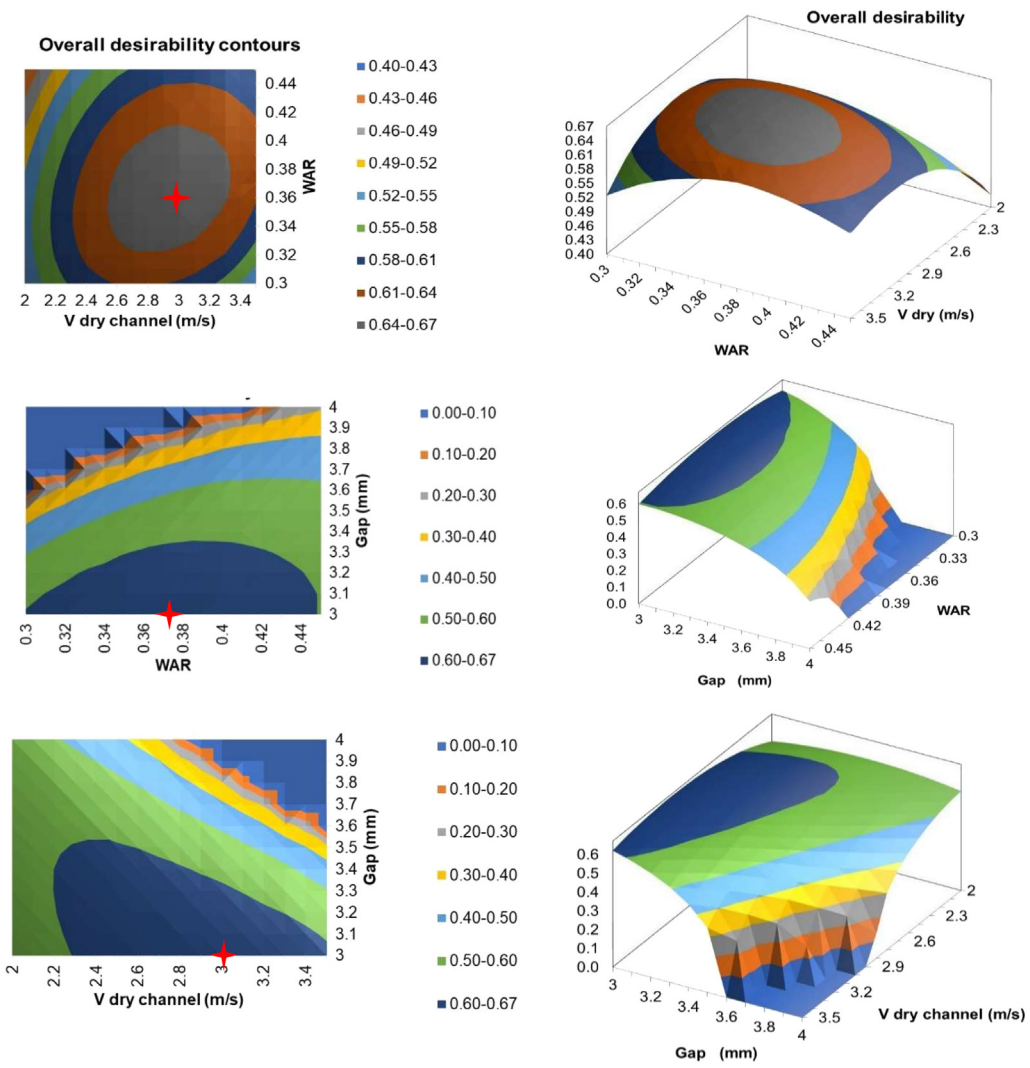

Fig. 14. Response surface and estimated contours of the overall desirability around the optimal operating conditions for Constantine city for the regenerative dew point cooler and for L = 0.6 m.

3 m/s and a channel gap of 3 mm which are the predicted optimal input parameters in this study. For these input parameters, the dew point efficiency is 17.7% lower than its maximum value of 85.2% , the COP is 22% lower than its maximum value of 46 and the cooling capacity of the exchanger is 10.2% lower than its highest value of 3030 W (these maximum values are shown in Fig. 13, around the optimal solution). These high values correspond to impractical situations where the overall desirability is zero or has a low value. Fig. 13 also shows that the overall desirability is very sensitive to the channel gap, since it is zero for gap values equal or greater than 3.8 mm. Then, it is sensitive to WAR. Its value drops from 0.56 to 0 when WAR decreases from 0.28 to 0.22.

These results are confirmed in Fig. 14, which shows overall desirability and its contours around the optimal values. Varying the inlet velocity between 2.8 and 3.2 m/s and WAR between 0.35 and 0.39 slightly decreases the overall desirability (less than 1%), while increasing the channel gap from 3 to 3.3 mm reduces the overall desirability to 0.611, or 7.1% less.

6.2. Combined parallel–regenerative dew point cooler for Constantine city

Fig. 15 shows the results of the multiple response optimization for the city of Constantine using the combined parallel–regenerative cooler. Optimal values of dew point efficiency, COP, and cooling capacity are 73%, 40 and 2900 W, respectively, for an overall desirability value of 0.717, which is 9% higher than the case of the regenerative dew point cooler. These values are evaluated for a WAR of 0.33, PAR of 0.58, relative parallel length of 15% and exchanger length of 0.6 m, dry air velocity of 2.9 m/s and channel gap of 3 mm, which are the predicted optimal input parameters for this case. Compared to the regenerative dew point cooler, at the same dew point efficiency, the COP and the cooling capacity are 5.3% and 5% higher, respectively. From Fig. 15, it can be noticed that the overall desirability is very sensitive to the channel gap and becomes zero for gap values equal to or greater than 4 mm. Subsequently, it is sensitive to WAR and Lparallel.

Fig. 16 shows the variations of the overall desirability and its contours as a function of WAR, PAR, and relative parallel length for channel length of 0.6 m and gap of 3 mm. Around the optimal input parameters, varying the PAR between 0.48 to 0.65, WAR between 0.31 and 0.35, and relative parallel length between 10 and 20% reduces overall desirability by less than 1%. It should be noted that the length of the parallel channel cannot be changed during exchanger operation.

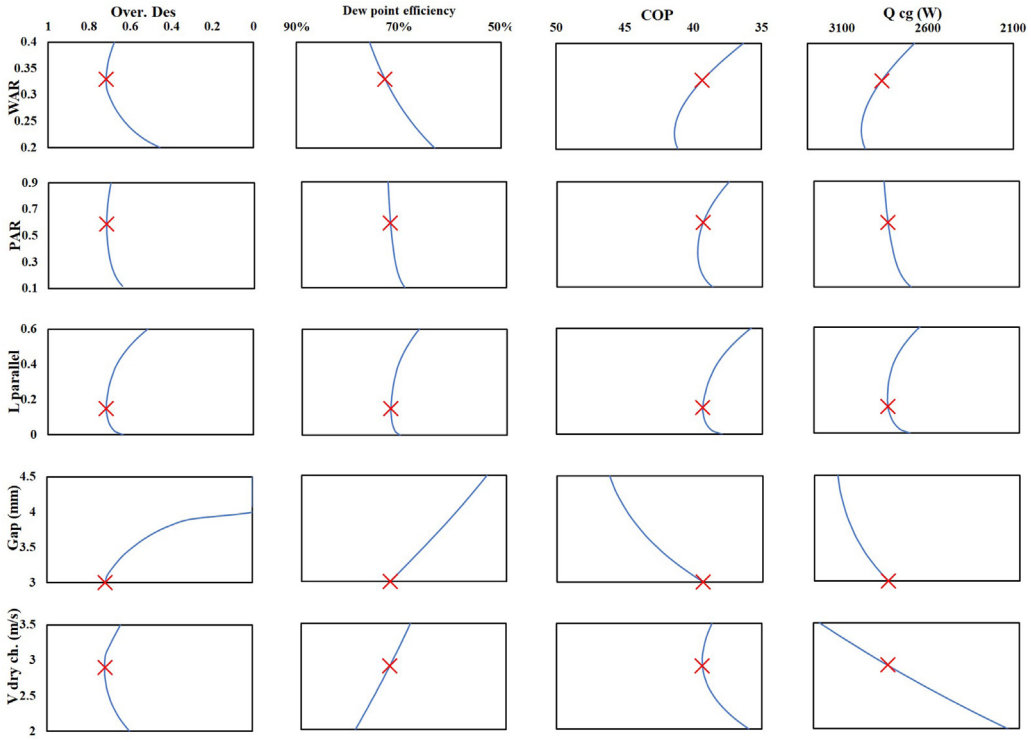

Fig. 15. Multiple response optimization using desirability function for Constantine city for the combined parallel counter-flow dew point cooler.

7. Optimization results for various climatic conditions in Algeria

Table 6 shows the optimization results for the three cities. For the regenerative cooler, substantial improvements are achieved between the base and optimal system. For the optimal case, the channel length and gap are reduced, and the velocity and WAR are increased. Checking the supply air temperature, it reaches 21.5 °C for Algiers, which means that the air is cooled about 10.5 °C to the outdoor conditions and suggests that dew point cooling technology is feasible for this city and can be combined with other cooling technologies to achieve lower cooling temperatures.

When comparing the combined configuration to the regenerative one (optimized cases), one can deduce that the use of the combined cooler provides no improvements in the dew point efficiency but increases the cooling capacity about 5%. However, these improvements can be counterbalanced by the combined system technology which is more complex than the regenerative system.

In order to understand differences between both configurations, latent heat and sensible heat fluxes in the wet channel and heat flux in the dry channel are computed. These are related by Eq. (5) and are defined as:

$$qdry = -U_d \left(T_d - T_{fw}\right) \tag{21}$$

$$qlatent = \rho\ h_m \left(g_{fw} - g_a\right) h_{fg} \tag{22}$$

$$qsensible = h_{aw} \left(T_{fw} - t_a\right) \tag{23}$$

Figs. 17 and 18 show heat flux in the dry channel as well as latent heat flux and sensible convective heat flux in the wet channel for the combined parallel counter flow configuration and for the counter flow configuration respectively for Constantine City (for the optimized cases).

These fluxes depend on temperature and humidity gradients. Heat flux qdry is always positive because the temperature of the air in the dry channel is always higher than water film temperature as shown in Fig. 10. The performance of the combined configuration is mainly due to the low variation of water temperature in the parallel part whereas in the counter flow exchanger water film temperature keeps increasing in the left part (as pointed by Hasan (2010) and Pandelidis et al. (2017)). The cooling capacity variation between both configurations can be explained by analyzing dry heat flux profiles in Figs. 17 and 18: in the left part, the combined configuration performs better and on the right part, the counter flow exchanger performs better because it has a higher working air ratio (WAR = 0.36; WAR = 0.33 for the combined configuration). The resulting cooling capacity is higher in the combined configuration (5%). The sensible convective heat in the wet channel is negative when heat transfer occurs from the air to the water film. While the profiles of sensible heat are similar in both configurations on the right part (counter flow part), the sensible heat flow changes direction and magnitude in the parallel part of the combined configuration meaning that some latent heat is used to cool air in the wet channel resulting in higher water consumption which is investigated in the next section.

Comparing humid coastal cities like Algiers to dry climate cities including Constantine and Ouargla, Table 6 indicates that the cooling capacity is strongly enhanced by 60% and 130% respectively. Fig. 19 compares the heat flux in the dry channel qdry for the three cities for the combined parallel-counter flow configuration. For Ouargla the cooling capacity is higher because its climate is drier and warmer (higher DBT–DPT from Table 5).

Similarly, the COP increases by 60% and 120% for Constantine and Ouargla respectively. COP growth is different than the cooling capacity because it also depends on the fan consumption. For Ouargla the velocity is higher than other cities leading to a higher consumption.

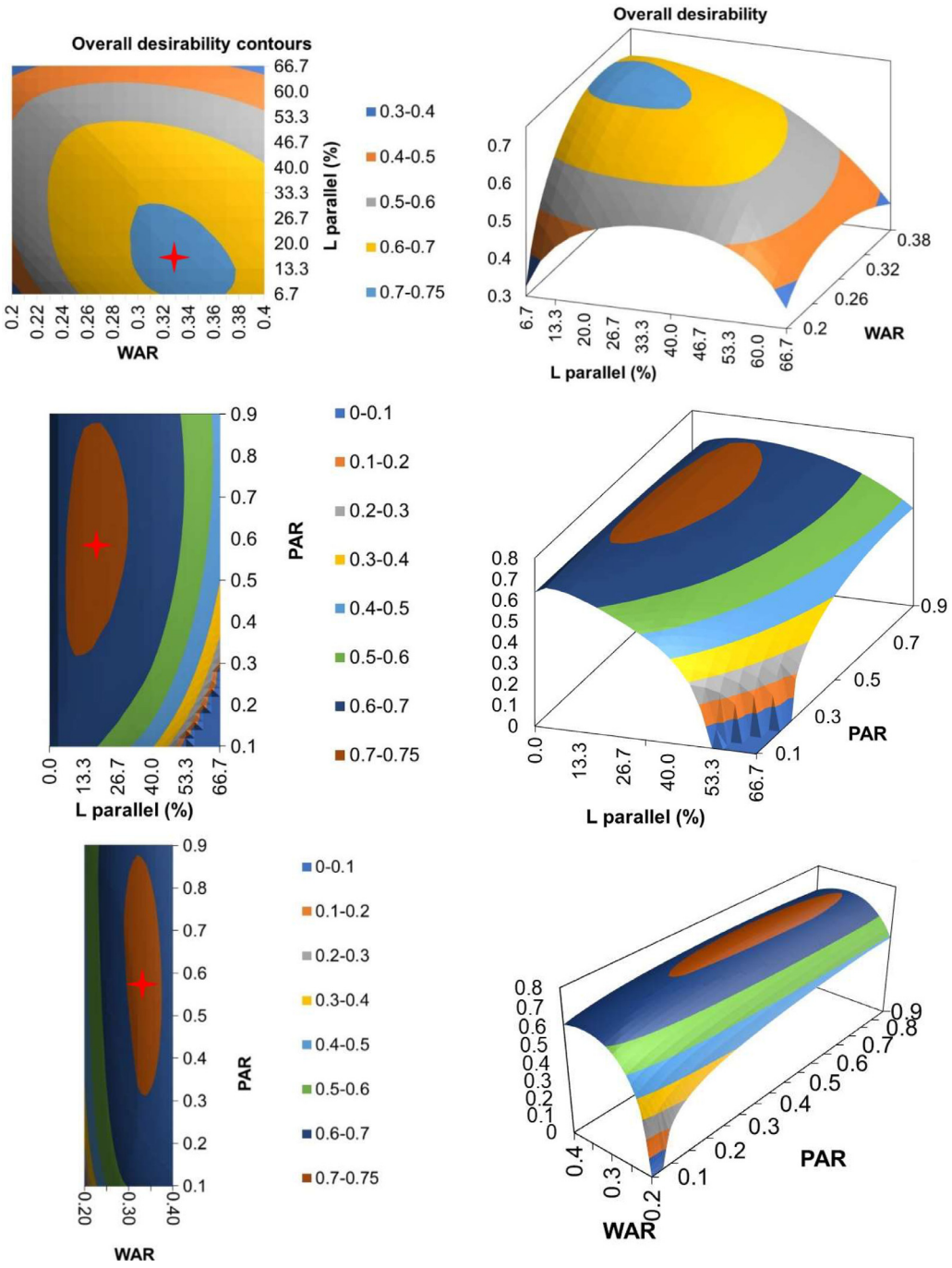

Fig. 16. Response surface and contours of the overall desirability around the optimal operating conditions for Constantine city for the combined dew point cooler, for L = 0.6 m and the gap H = 0.003 m.

8. Water consumption

Regarding the optimization results for different climate zones in Algeria, the best case is relevant to Ouargla. The city is situated in Algerian Sahara with low rainfall and water scarcity, the prediction of the water consumption is necessary.

Table 7 shows the theoretical water consumption for the optimal design for both configurations in the three studied cities. It is computed according to the following formula:

$$\dot{m}_w = \dot{m}_d \left[PAR\,(g_{a,in} - g_{a,out})_{pp} + WAR(g_{a,in} - g_{a,out})_{regp} \right] \quad (24)$$

Comparing the two configurations, for the three cities, the consumption of the combined cooler is higher than that of the regenerative one with an increase of 43% in Algiers, 42% in Ouargla and 38% in Constantine. It is also noted that the water consumption in Ouargla is the highest since its climate is drier, the air velocity is higher as well as the PAR (parallel air flow ratio). Ouargla presents a 137.5% and 135% higher water consumption than Algiers for the regenerative and combined coolers respectively. This is due to the humid climate of Algiers.

Fig. 20 compares the intensity of water evaporation along the channel for both configurations. While on the right part both configurations are similar, the intensity of evaporation is higher in the combined mode due to high humidity ratio gradient in the

Table 6
Initial, optimum design parameters and improvements in objective functions for the three cities.

Parameters		Cities		
		Constantine	Ouargla	Algiers
Decision variables for the base system (regenerative)	L (m)	0.8	0.8	0.8
	Gap (mm)	4	4	4
	V (m/s)	2	2	2
	WAR	0.25	0.25	0.25
Performance of the base system	COP	34	50	21.7
	ε_{dp} (%)	65.3	68	69
	$Q_{cooling}$ (W)	1950	2850	1240
	Tsupply (°C)	20	22.1	22.6
	Q_{room} (W)	805	520	454
Decision variables for the optimal design (regenerative)	L (m)	0.6	0.6	0.6
	Gap (mm)	3	3	3
	V (m/s)	3	2.94	2.9
	WAR	0.363	0.36	0.365
Performance of the optimal design (regenerative)	COP	37.5	54.9	24
	ε_{dp} (%)	72.5	73.5	76.7
	$Q_{cooling}$ (W)	2750	3950	1715
	Tsupply (°C)	18.3	20.32	21.54
	Q_{room} (W)	1285	954	723
Performance improvement (compared to base system)	COP (%)	10.2	9.8	10.6
	ε_{dp} (%)	11	8	11.1
	$Q_{cooling}$ (%)	41	38.6	38.3
	Q_{room} (%)	60	83.5	59
Decision variables for the optimal design (combined cooler)	L (m)	0.6	0.6	0.6
	Gap (mm)	3	3	3
	V (m/s)	2.9	3.1	2.9
	WAR	0.326	0.336	0.326
	PAR	0.58	0.62	0.6
	Lparallel	0.15	0.13	0.15
Performance of the optimal design (combined cooler)	COP	39.5	55.9	25
	ε_{dp} (%)	73	73.2	76.8
	$Q_{cooling}$ (W)	2900	4200	1820
	Tsupply (°C)	18.3	20.42	21.53
	Q_{room} (W)	1350	1010	780
Performance improvement (combined cooler compared to regenerative case)	COP (%)	5.3	1.8	4.2
	ε_{dp} (%)	0.5	−0.4	0.1
	$Q_{cooling}$ (%)	5.5	6.3	6.1
	Q_{room} (%)	5	5.9	7.9

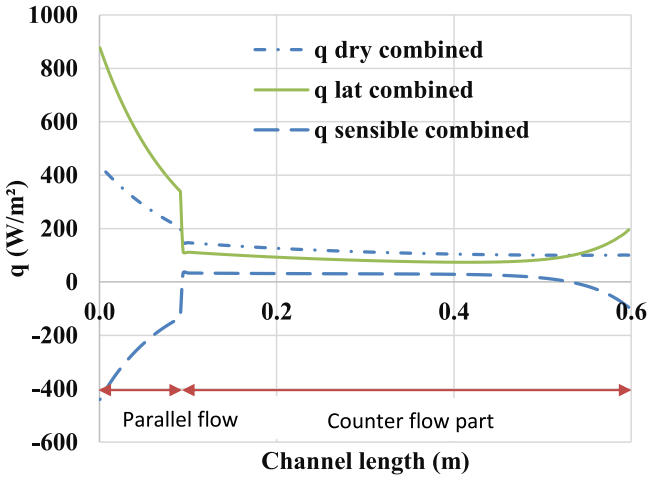

Fig. 17. Variation of heat flux density along the channel for the optimized combined parallel counter flow configuration in Constantine city.

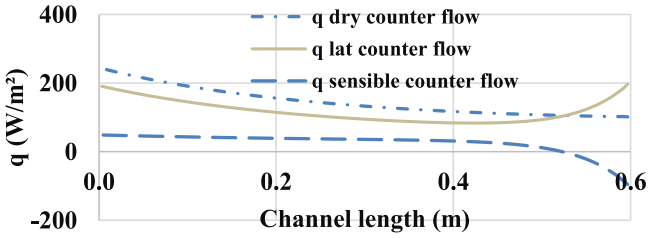

Fig. 18. Variation of heat flux density along the channel for the optimized counter flow configuration in Constantine city.

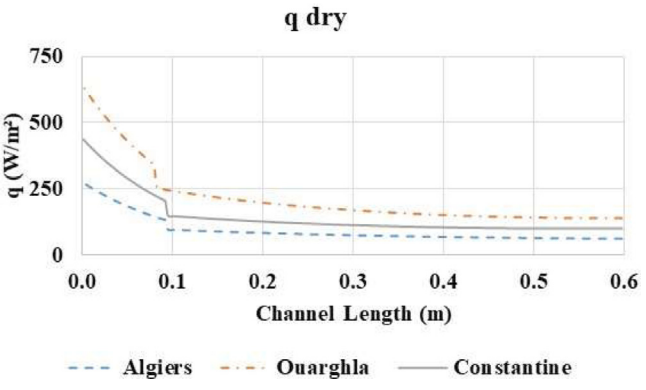

Fig. 19. Variation of heat flux density along the channel for.

wet channel between water film and wet air as well as the high air flow rate. This results in a higher water consumption (38%).

9. Conclusion

The multi objective response of two configurations of the dew point evaporative cooler via GPS/PSO hybrid optimization was

Table 7
Water consumption for the three cities.

City	Regenerative dew point cooler (kg/h)	Combined dew point cooler (kg/h)
Constantine	5.2	7.2
Ouargla	7.6	10.8
Algiers	3.2	4.6

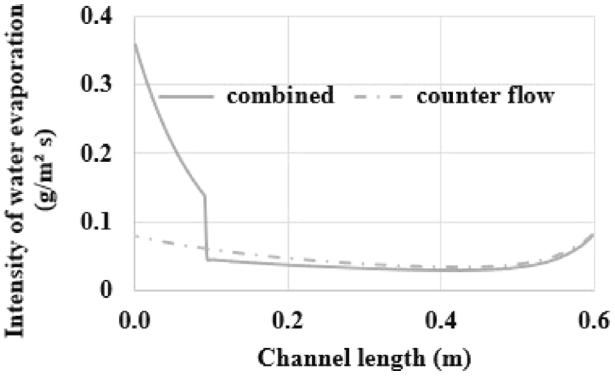

Fig. 20. Intensity of water evaporation along the wet channel for both configurations for Constantine city.

performed using the desirability approach. The studied configurations are the regenerative dew point cooler and the combined parallel counter flow cooler. A numerical model was implemented in the SPARK simulation environment and was validated with experimental data from the literature. The optimization was performed with GenOpt and allowed to compare both configurations from a thermodynamic point of view and for three climatic conditions in Algeria. It is noticed that all the thermodynamic parameters must be considered in the comparison and not only one parameter. The following are the key findings:

(a) The overall desirability, for the dew point evaporative cooler predicted in Constantine city, depends on the channel gap, which should be less than 3.8 mm. The optimum values for dew point efficiency, COP and cooling capacity are 72.4%, 37.5, and 2750 W respectively for a value of desirability of 0.658. This corresponds to operating conditions of WAR of 0.363, length of 0.6 m, dry air velocity of 3 m/s and a channel gap of 3 mm.
(b) For the same city, the combined parallel–regenerative cooler has optimal efficiency, COP and cooling capacity of 72.6%, 40 and 2900 W respectively, for a desirability value of 0.717, as well as WAR of 0.33, PAR of 0.58, relative parallel length of 15%, an exchanger length of 0.6 m, dry air velocity of 2.9 m/s and a channel gap of 3 mm.
(c) Comparing humid coastal cities like Algiers to dry climate cities including Constantine and Ouargla, it can be noticed that the cooling capacity is strongly enhanced by 60% and 130% respectively. Similarly, the COP increases by 60% and 120% respectively, yielding the necessity of the proposed study.
(d) Comparing the regenerative dew point and the combined parallel counter flow configurations for the optimized cases, in the combined configuration, the cooling capacity is improved by about 5% at equal dew point efficiency for all three cities. However, the combined dew point cooler consumes more water than the regenerative cooler (about 40%) which can restrict the use of this kind of configuration especially in a desert climate like Ouargla City where water is extremely scarce.

Further research direction can focus on coupling the system with a building model with an appropriate regulation strategy as well as modeling other dew point coolers configurations.

CRediT authorship contribution statement

A.F. Boudjabi: Conceptualization, Methodology, Writing – original draft, Investigation, Visualization. **C. Maalouf:** Conceptualization, Methodology, Software, Funding acquisition. **T. Moussa:** Methodology, Software, Writing – editing. **D. Abada:** Conceptualization, Investigation. **D. Rouag:** Conceptualization, Funding acquisition. **M. Lachi:** Methodology, Writing. **G. Polidori:** Conceptualization, Methodology, Writing – editing.

Declaration of competing interest

The authors declare that they have no known competing financial interests or personal relationships that could have appeared to influence the work reported in this paper.

Acknowledgments

This work is part of the results of a scientific research cooperation between France and Algeria and supported by the Hubert Curien Partnership (PHC TASSILI).

Appendix

A.1. Horizontal counter flow dew point evaporative cooler

In this section, additional validation of the horizontal flow dew point cooler is performed. The considered parameters are the inlet air velocity and the working air ratio.

A.1.1. Effect of inlet air velocity

The supply air temperature and the working air temperature are predicted as a function of the intake air velocity. Compared to the experimental values, the calculations show good agreement and an average deviation of less than 1.2% for the supply air temperature. A larger difference of about 2 °C between the numerical and experimental values is reported for the working air temperature.

At air velocity below 1.3 m/s, the heat transfer is improved due to a longer residence time, at the detriment of a lower cooled air flow rate delivered to the building, nevertheless, the gain in cooling temperature is only 0.5 °C to 1 °C, as seen on Fig. A.1.1. It is noticed that above 1.5 m/s air flow rate, the supply air temperature is not sufficiently influenced.

A.1.2. Effect of working air ratio

In Fig. A.1.2., it can be seen that the discrepancy between the calculated and measured values is acceptable. In the dry channel, the deviation of the supply air temperature is estimated to be between ±0.34 °C and ±1.4 °C, 0.4% at minimum and 8.8% at maximum. In the wet channel, the deviation is slightly higher, 5% with a temperature difference of ±0.3 °C to ±2.15 °C. Moreover, the supply air temperatures as well as the working air temperature decrease considerably, when the working air ratio increases. The drop becomes more stable above a ratio of 0.6.

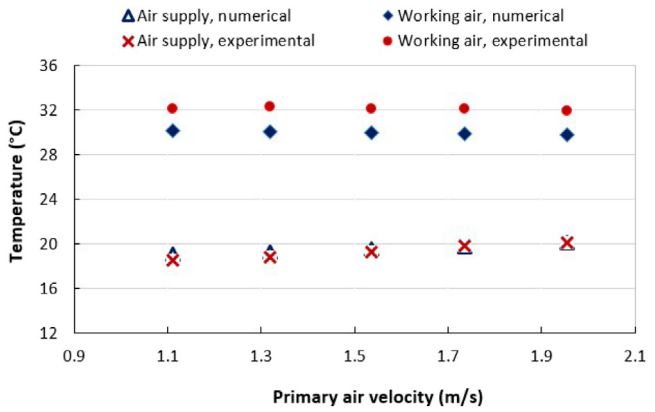

Fig. A.1.1. Effect of primary air velocity on air supply and working air temperatures.

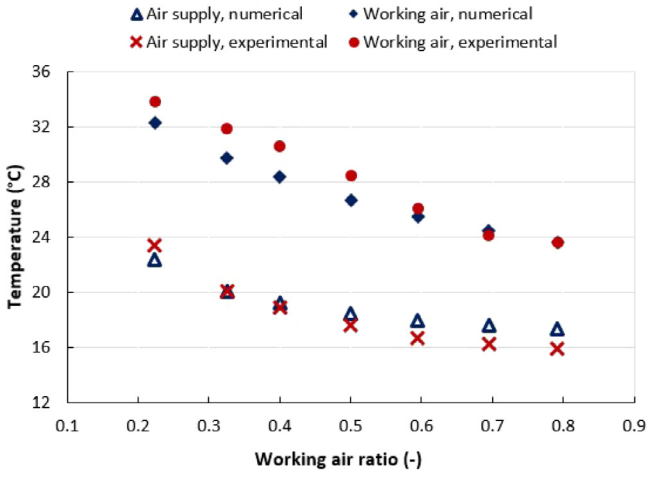

Fig. A.1.2. Effect of working air ratio on air supply and working air temperatures.

Table A.1
Experimental setup parameters.

Channel's length	1200 mm
Channel's width	80 mm
Channel's gap	5 mm
Water film temperature	28 °C
Airflow rate	60 l/h
Working air ratio	0.33

A.2. Vertical dew point evaporative cooler

Riangvilaikul and Kumar (2010) conducted an experimental study of a dew point evaporative air cooler in a vertical arrangement, as shown in Fig. A.2.1. The system specifications are summarized in Table A.1. The experimental data are as follows: inlet air temperature varied from 25 °C to 45 °C, inlet air humidity from 6.9 g/kg to 26.4 g/kg and intake air velocity from 1.1 m/s to 6 m/s.

Fig. A.2.2 illustrates the results of the numerical model and the experimental data. The numerical results are in good agreement with the experimental data, with the discrepancy in most points varying from 0.5% to 4%, with a few points giving an error of more than 4% and up to 9.1%.

In the illustration in Fig. A.2.3., the system efficiency is plotted, the intake air velocity is varying from 1.11 m/s to 6 m/s, the inlet temperature is set to 34 °C and calculations are performed for

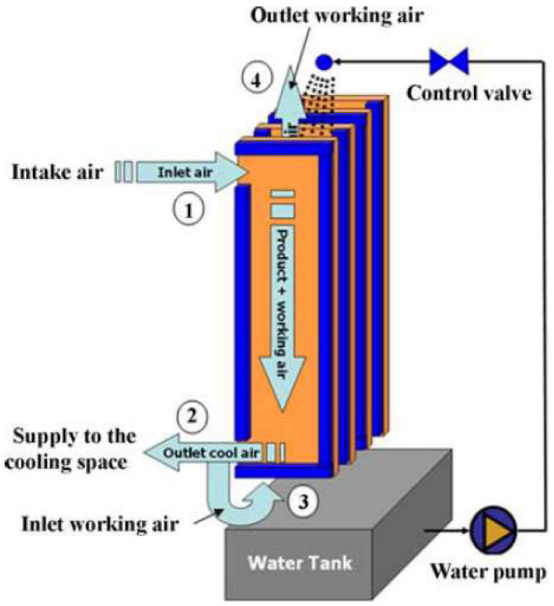

Fig. A.2.1. Experimental setup of the evaporative cooling system (Riangvilaikul et al., 2010).

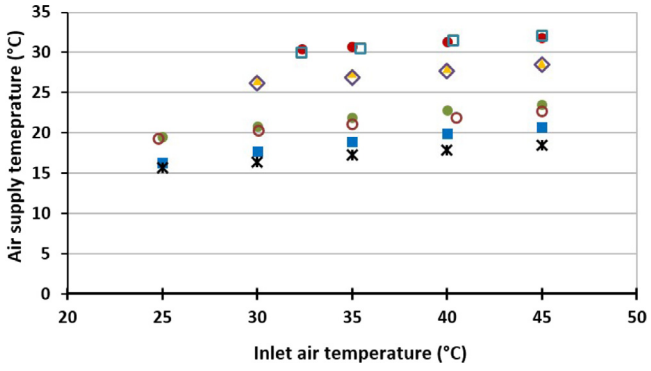

Fig. A.2.2. Air supply temperature for different external conditions.

Table A.2
Operating conditions.

Channel's length	1000 mm
Channel's width	1000 mm
Channel's gap	3 mm
Inlet air velocity	3 m/s
Inlet air temperature	30 °C
Relative humidity	45%
$X_{parallel}$	0.1 – 0.9

two air humidity values of 11.2 g/kg and 19 g/kg. The wet bulb and dew point efficiency graphs of the experimental cases are in a good agreement with the numerical results (discrepancy from 1.6% to 2.7% at most).

A.3. Combined parallel–regenerative

Pandelidis et al. (2017) performed numerical studies on a combined parallel–regenerative exchanger using the modified ε-NTU method (Fig. A.3.1.). The length of parallel flow section, the working air ratio in the parallel part and the working air ratio in the counter-current part are designed by $X_{parallel}$, w_3/w_1 and w_2/w_1 respectively. The operating conditions are summarized in Table A.2.

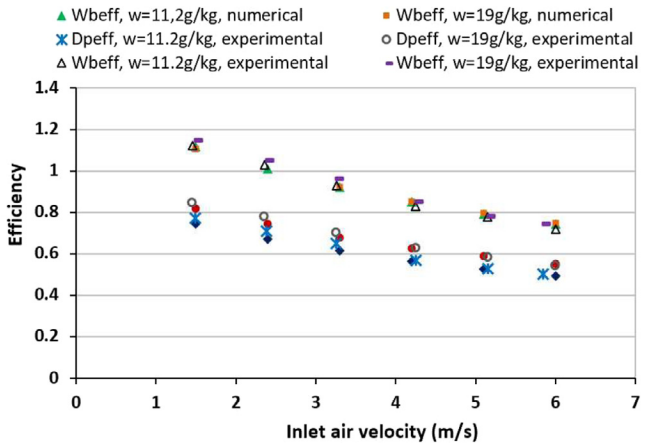

Fig. A.2.3. System effectiveness for different intake air velocity.

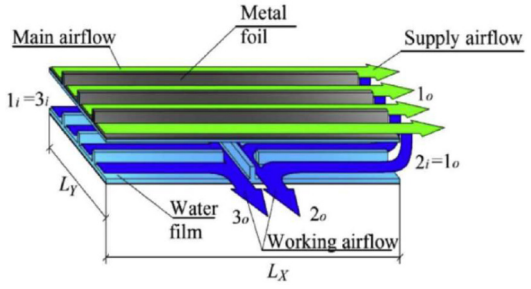

Fig. A.3.1. Schematic combined parallel–regenerative evaporative exchanger (Pandelidis et al., 2017).

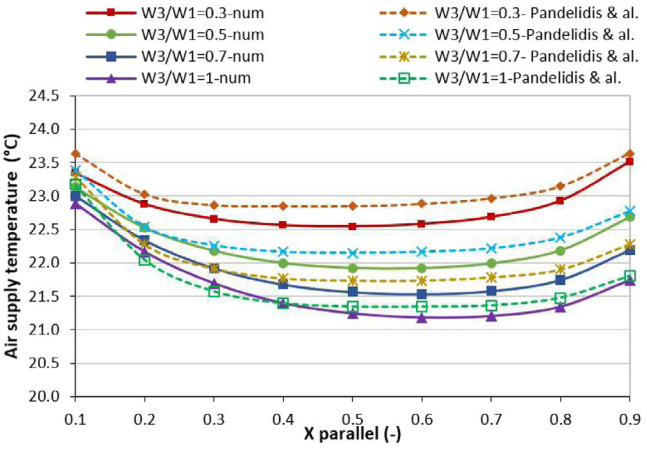

Fig. A.3.2. Air supply temperature versus $X_{parallel}$ and w_3/w_1 for $w_2/w_1 = 0.1$.

In this analysis, the regenerative part w_2/w_1 is set to 10%, 30 and 50% of the primary airflow rate, so, the calculations are for predicting supply air temperatures according to the different working air ratios in the parallel part w_3/w_1.

The curves on Fig. A.3.2. show the supply air temperature for $w_2/w_1 = 0.1$ and different ratios of w_3/w_1. There is a good agreement between both models. For amounts of w_3/w_1: 0.3, 0.5, 0.7 and 1, the deviation is satisfactory within 3.3%, 4.2%, 1.6% and 2.2% respectively.

In the case of regenerative air ratio of 30% (see Fig. A.3.3.), the average error is less than 0.4% for all air supply temperatures. The

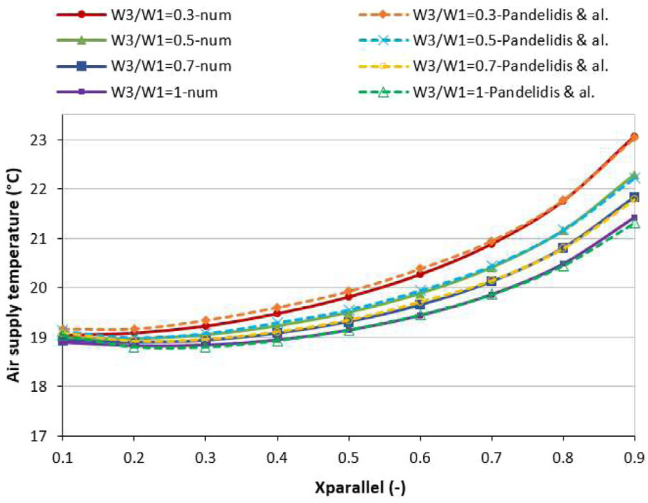

Fig. A.3.3. Air supply temperature versus $X_{parallel}$ and w_3/w_1 for $w_2/w_1 = 0.3$.

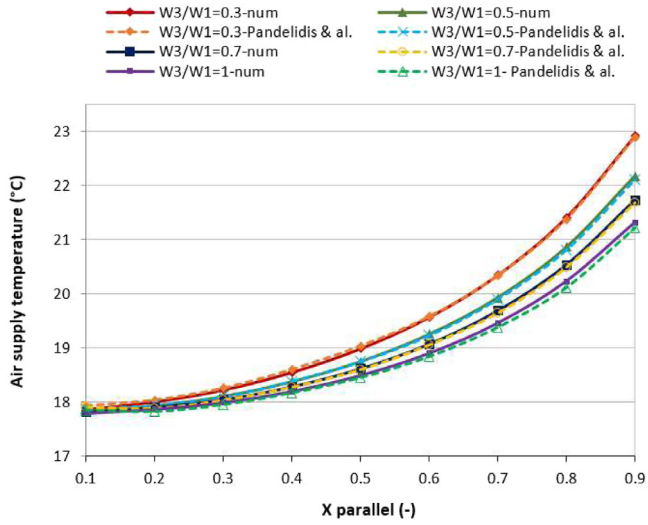

Fig. A.3.4. Air supply temperature versus $X_{parallel}$ and w_3/w_1 for $w_2/w_1 = 0.5$.

mean error in the case of $w_2/w_1 = 0.5$ (see Fig. A.3.4.), is less than 0.2%.

References

Algerian Energy Ministry, 2017. Bilan énergétique national 2016. Algeria, Edition, pp. 20-21.

Algerian Energy Ministry, 2019. Bilan énergétique national 2018. Algeria, Edition, pp. 22-23.

Anisimov, S., Pandelidis, D., 2015. Theoretical study of the basic cycles for indirect evaporative air cooling. Int. J. Heat Mass Transf. 84, 974–989.

Anisimov, S., Pandelidis, D., Danielewicz, J., 2014. Numerical analysis of selected evaporative exchangers with the maisotsenko cycle. Energy Convers. Manag. 88, 426–441.

Anisimov, S., Pandelidis, D., Danielewicz, J., 2015. Numerical study and optimization of the combined indirect evaporative air cooler for air conditioning systems. Energy 80, 452–464.

Anisimov, S., Zuchowicki, J., 2005. Renewable energy utilization in indirect evaporative air coolers of air conditioning system. In: Proceedings of International Conference. TSCE'05, Egypt, 15-18 April pp. 2-7.

Boukhanouf, R., Ibrahim, H.G., Alharbi, A., Kanzari, M., 2014. Investigation of an evaporative cooler for buildings in hot and dry climates. Clean Energy Technol. 2 (3), 221–225.

Camargo, J.R., Ebinumca, C.D., Silveira, J.L., 2003. Thermoeconomic analysis of an evaporative dissicant air conditioning system. Appl. Therm. Eng. 23, 1537–1549.

Derringer, G., Suich, R., 1980. Simultaneous optimization of several response variables. J. Qual. Technol. 12, 214–219.
Duan, Z., 2011. Investigation of a Novel Dew Point Indirect Evaporative Air Conditioning System for Buildings (Ph.D. thesis). University of Nottingham, p. 189.
Guangya, Z., Weiwei, C., Shihua, L., 2019. Modelling of a dew point effectiveness correlation for maisotsenko cycle heat and mass transfer. Chem. Eng. Process. 145 (07665).
Ham, S.W., Jeong, J.W., 2016. Dphx (dew point evaporative heat exchanger): System design and performance analysis. Energy 101, 132–145.
Hasan, A., 2010. Indirect evaporative cooling of air to a sub-wet bulb temperature. Appl. Therm. Eng. 30, 2460–2468.
Holman, J.P., 2010. Heat Transfer, tenth ed. McGraw-Hill, Inc., 1221QC320.H64.
Jafarian, H., Sayyaadi, H., Torabi, F., 2017a. A numerical model for a dew point counter-flow indirect evaporative cooler using a modified boundary condition and considering effects of entrance regions. Int. J. Refrig. 84, 33–35.
Jafarian, H., Sayyaadi, H., Torabi, F., 2017b. Modeling and optimization of dew point evaporative coolers based on a developed GMDH-type neural network. Energy Convers. Manag. 143, 49–65.
Kashyap, S., Sarkar, J., Kumar, A., 2020. Comparative performance analysis of different novel regenerative evaporative cooling device topologies. Appl. Therm. Eng. 176, 115474.
Lee, J., Lee, D.Y., 2013. Experimental study of a counter flow regenerative evaporative cooler with finned channels. Int. J. Heat Mass Transf. 65, 173–179.
Lertsatitthanakorn, C., Rerngwongwitaya, S., Soponronnarit, S., 2006. Field experiments and economic evaluation of an evaporative cooling system in a silkworm rearing house. Biosyst. Eng. 93 (2), 213–219.
Lin, J., Wang, R., Li, C., Wang, S., Long, J., Cha, K.J., 2020. Towards a thermodynamically favorable dew point evaporative cooler via optimisation. Energy Convers. Manag. 203, 112224.
Liu, Y., Li, J.M., Yang, X., 2019. Two-dimensional numerical study of a heat and mass exchanger for a dew-point evaporative cooler. Energy 168, 975–988.
Maalouf, C., Moussa, T., Boudjabi, A.F., Abada, D., Polidori, G., Saffidine-Rouag, D., Wultz, E., 2018. Numerical study and design of a dew point evaporative cooler for buildings. In: Proccedings of EENVIRO, Cluj Napoca, Romania, October.
Maisotsenko, V., Gillan, L.E., Heaton, T.L., Gillan, A.D., 2003. Method and plate apparatus for dew point evaporative cooler. U.S. Patent US6581402 B2.
Pakari, A., Ghani, S., 2019. Comparison of 1D and 3D heat and mass transfer models of a counter flow dew point evaporative cooling system: Numerical and experimental study. Int. J. Refrig. 99, 114–125.
Pandelidis, D., Anisimov, S., Rajski, K., Brychcy, E., M., Sidorczyk., 2017. Performance comparison of the advanced indirect evaporative air coolers. Energy 135, 138–152.
Pengfei, L., Xinyu, L., 2015. Simulation on three dimensional laminar properties of dew point evaporative cooling in plate heat exchanger. In: Proceedings of 3rd International Conference on Mechanical Engineering and Intelligent Systems ICMEIS, Singapore.
Ren, C., Yang, H., 2006. An analytical model for the heat and mass transfer processes in indirect evaporative cooling with parallel/ counter flow configurations. Int. J. Heat Mass Transf. 49, 617–627.
Riangvilaikul, B., Kumar, S., 2010. An experimental study of a novel dew point evaporative cooling system. Energy Buid. 42, 637–644.
Sohani, A., Sayyaadi, H., Hosseini, N.M., 2018. Comparative study of the conventional types of heat and mass exchangers to achieve the best design of dew point evaporative coolers at diverse climatic conditions. Energy Convers. Manag. 158, 327–345.
Sowell, E.F., Haves, P., 2001. Efficient solution strategies for building energy system simulation. Energy Build. 33, 309–317.
Stoitchkov, N.J., Dimitrov, G.I., 1998. Effectiveness of crossflow plate heat exchanger for indirect evaporative cooling. Int. J. Refrig. 21 (6), 463–471.
Wetter, ., 2000. Design Optimization with GenOpt. Building Energy Simulation User News, https://simulationresearch.lbl.gov/wetter/download/userNews-2000.pdf.
Wetter, M., 2009. GenOpt, a Generic Optimization Program, Version 3.0.0 User Manual 3.0.0. Technical Report LBNL-2077E, Berkeley, CA.
Zhan, C., Duan, Z., Zhao, X., Smith, S., Jin, H., Riffat, S., 2011. Comparative study of the performance of the M-cycle counter-flow and cross-flow heat exchangers for indirect evaporative cooling- paving the path toward sustainable cooling of buildings. Energy 36 (12), 6790–6805.
Zhao, X., Li, J.M., Riffat, S.B., 2008. Numerical study of a novel counter-flow heat and mass exchanger for dew point evaporative cooling. Appl. Therm. Eng. 28, 1942–1951.